Removal of nickel through sulfide precipitation and characterization of electroplating wastewater sludge

Sarah Jerroumi, Mohammed Amarine, Hassan Nour, Brahim Lekhlif and Jamal Eddine Jamal

ABSTRACT

This work consists of the removal of nickel by sulfide precipitation from industrial electroplating wastewater and characterization of the produced sludge. Tests are carried out in a perfectly stirred batch reactor on electroplating industrial solution and synthetic solution prepared in the laboratory. The aim is to evaluate the impact of complexing agents formed during precipitation of metal ions in the industrial effluent. The concentration of nickel in both solutions is 100 mg/L. The operating conditions for the sulfide precipitation process are optimized: pH, molar ratio $[S^=]/[Ni^{2+}]$ and dosage of $S^=$ ions. For an initial pH of 5 and an equimolar ratio of $[S^=]/[Ni^{2+}]$:1/1, the results show that the removal efficiency of Ni^{2+} ions is approaching 91 and 94% for industrial and synthetic solutions, respectively. Otherwise, for the same pH value in supersaturation conditions ($[S^=]/[Ni^{2+}]$:1.5/1), the removal efficiency is approaching 62 and 92% for industrial and synthetic solutions, respectively. For an effective metal removal, the optimal dosage of sulfide ions was evaluated. For 33 mg/L of $S^=$, the removal efficiency of Ni^{2+} is approximately 90%. The resulting sludge has been characterized by X-ray diffractometry, scanning electron microscopy, infrared spectroscopy and thermal analysis. It consists essentially of millerite and nickel oxide.

Key words | millerite, nickel, nickel sulfide, precipitation, sludge, supersaturation

Sarah Jerroumi (corresponding author)
Hassan Nour
Jamal Eddine Jamal
Department of Chemistry, Faculty of Sciences Ain Chock,
Hassan II University,
B.P 5366, Casablanca,
Morocco
E-mail: sarah_jerroumi@hotmail.com

Sarah Jerroumi
Mohammed Amarine
Brahim Lekhlif
Department of Water Treatment and Climate Change, Hassania School of Public Works,
Hassan II University,
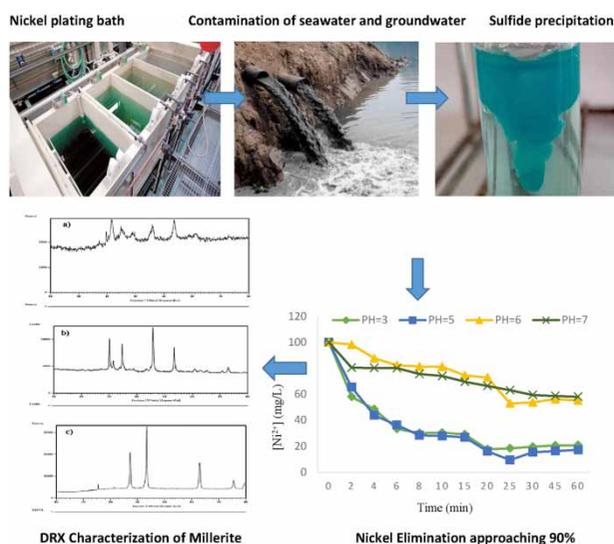B.P 5366, Casablanca,
Morocco

Mohammed Amarine
Laboratory of Water Chemistry,
Pasteur Institute of Morocco,
1, Place Louis Pasteur, Casablanca, 20360,
Morocco

HIGHLIGHTS

- The recovery of nickel precipitate was improved when the initial pH of the solution, with stoichiometric ratio ($[S=]/[Ni^{2+}]$: 1/1), was set to 5 giving a nickel abatement rate above 98%.
- Tests carried out with a ratio $[S=]/[Ni^{2+}]$ equal to 1.5/1 at pH 5 showed that the excess of sulphide ions reduces the efficiency of nickel removal due to the displacement of the equilibrium of the precipitation reaction to more HS- and H2S and to the rapid increase of pH which is related to the formation of aqueous polysulfide complexes.
- Sulphide precipitation can be used to precipitate nickel as millerite (NiS). The result of heat treatments and analysis of the composition and morphology shows that it is a recoverable material and guarantees compliance with environmental regulations.

GRAPHICAL ABSTRACT

INTRODUCTION

Heavy metal pollution has become a major environmental problem receiving growing attention in recent years. Most industrial sectors generate contaminated wastewater with metallic elements, causing serious environmental damage (Wei *et al.* 2019). An example would be the electroplating industry releasing effluents mainly issuing from metal products' manufacture. Environmental contamination by heavy metals (arsenic, chromium, zinc, nickel, etc.) has been reported in various countries such as China, Morocco, Mexico, United States, India, Indonesia, Bangladesh, Thailand, etc. (Wakida *et al.* 2008; Babu *et al.* 2009; Taouil *et al.* 2014; Wang & Chen 2015).

A number of studies in humans and animals suggest that exposure to soluble nickel salts leads to systemic effects on the kidneys, neonatal mortality and effects on the immune system. The kidney is the main target organ for both animals and humans (Lentini *et al.* 2017). Several experimental and epidemiological studies have shown that nickel is genotoxic and has a fatal effect on the indigenous aquatic biota (Binet *et al.* 2018).

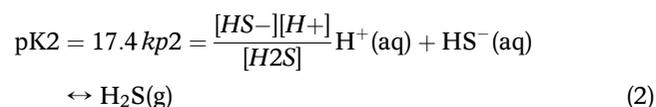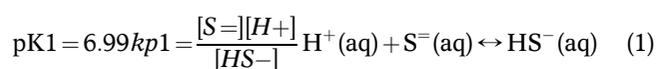In the last few decades, many technologies have been applied to the treatment of metal-laden effluent such as ion exchange, electrocoagulation, chemical precipitation, adsorption, and solvent extraction. Their advantages and limitations have been evaluated by several authors (Coman *et al.* 2013; Mnasri-Ghnimi & Frini-Srasra 2019; Jerroumi *et al.* 2019; Pan & An 2019; Wu 2019; Sunder *et al.* 2020).

Hydroxide precipitation treatment is the most used technique for industrial discharges. The process is simple and cost-effective (Brbooti *et al.* 2011). However, a high volume and poor dewatering properties characterize the precipitated sludge, which increases handling and disposal costs. Also, optimum precipitation takes place generally at pH values between 10 and 11, which may require neutralization post-treatment (Sampaio *et al.* 2009). Otherwise, the application of sulfide precipitation proves to be a relevant and promising technology with various merits over hydroxide precipitation, with higher selectivity for nickel removal, faster reaction rates, better dewatering properties of sludge, and lower solubility of precipitate (Lewis 2010). Even at acidic pH, most heavy metal sulfides have very low solubilities. For example, the solubility product Ksp of NiS is 1×10^{-22} (Zelekew & Kuo 2017).

Sulfides can come from either a solid (CaS, FeS), soluble salt (Na$_2$S, NaHS) or gaseous source (H$_2$S). However, the dosing of S$^=$ is not always easily controllable because of

the very low solubility of the produced metal sulfides. Indeed, many authors have shown the influence of sulfide ion concentration on the elimination of metals (Cu, Fe, Ni, etc.). They conclude that the removal efficiency of metals is highly dependent on the dosage of $S^=$ ions. They note that an excess of $S^=$ ions leads to the formation of polysulfide complexes and an insufficient $S^=$ dosage results in an incomplete precipitation (Cao *et al.* 2009).

During the reaction of sulfide precipitation, the sulfide reacts with H^+ of the solution, especially in acidic solutions, according to reactions (1) and (2):

$$pK1 = 6.99 \; kp1 = \frac{[S^=][H+]}{[HS-]} \; H^+(aq) + S^=(aq) \leftrightarrow HS^-(aq) \quad (1)$$

$$pK2 = 17.4 \; kp2 = \frac{[HS-][H+]}{[H2S]} \; H^+(aq) + HS^-(aq)$$
$$\leftrightarrow H_2S(g) \quad (2)$$

$$Ni^{2+} + S^= \leftrightarrow NiS \quad (3)$$

$$Ni^{2+} + HS^- \leftrightarrow NiS + H^+ \quad (4)$$

The problem of resource scarcity has encouraged research on waste valorization. Industrial sludge usually contains heavy metal, which enhances its dangerousness and treatment difficulty (Shi *et al.* 2018). Sulfide sludge is commonly generated from sulfide precipitation of nickel in wastewater. Therefore, the valorization of this material would have a higher industrial interest. Currently, the main disposal routes include landfills, incineration and pyrolysis (Xu *et al.* 2015). These traditional methods have resulted in wasting of resources and risk of secondary pollution of the environment (Panepinto *et al.* 2016). The present work aims to improve the efficiency of nickel elimination by sulfide precipitation and establish a series of tests on electroplating effluent with the goal of optimizing the relevant parameters such as the pH, the molar ratio $[S^=]/[Ni^{2+}]$ and the dosage of sulfides. The same sulfide precipitation protocol is applied to synthetic water. In this paper, we report the results of characterization of metallic sludge by several techniques, such as X-ray diffraction (XRD), scanning electron microscopy (SEM), infrared spectroscopy (IR) and thermal analysis (TGA/DTA), in order to provide detailed information about the crystallographic structure, chemical composition and physical properties of sulfide sludge.

MATERIALS AND METHODS

Sulfide precipitation tests were performed in a pyrex-reactor. The treated volume of nickel-rich effluent was 500 mL (100 mg/L of Ni^{2+}). Synthetic nickel-rich waters were prepared from $NiCl_2$, $6H_2O$. Sodium sulfide salts (Na_2S) were used as the source of sulfide ions ($S^=$) and added to the volume of nickel-rich solution. The mixture was stirred at moderate speed (30 rpm) with a magnetic stirrer. The pH adjustment was carried out with 0.1 M HCl or 0.1 M NaOH. All of the chemicals were of analytical grade supplied by Scharlau and all solutions were prepared using distilled water.

The first test studied the effect of initial pH (3, 5, 6, 7) of the mixture (nickel-rich solution and sulfide solution) with stoichiometric ratio between nickel and sulfide ($1[S^=]:1[Ni^{2+}]$) on the nickel removal.

The second test studied the effect of molar ratio between nickel and sulfide ($1.5[S^=]:1[Ni^{2+}]$) on the nickel removal. The initial pH of the mixture was fixed on the optimum value giving the maximal nickel ions' removal rate in the first test.

The third test studied the effect of sulfide ions' concentration on the nickel removal.

During each test, a 20 mL sample was taken every 2 minutes for the first 10 minutes of the reaction, then, every 5 minutes for the next 30 minutes, and every 15 minutes for the last 30 minutes. The samples were filtered using membrane filters (0.45 μm) and stored with a drop of concentrated nitric acid (70%) (Aldrich) for nickel analyses. The nickel concentration was measured using an atomic absorption spectrometer (AA-7000).

The yield of nickel removal can be calculated as follows:

$$R(\%) = \frac{Ci - Cf}{Ci}$$

where Ci is the initial concentration and Cf is the final concentration.

The sludge generated from sulfide precipitation at optimal conditions was a black powder whose mass weight was approaching 48.93 mg. It was filtered and dried at

150 °C for 24 hours before characterization. The X-ray diffraction analysis of the sludge was performed by D8 ADVANCE powder diffractometer coupled to a computer operating system. The spectra were recorded at $10° < 2\theta < 80°$. The diffractograms were processed using HighScore software which is based on data from JCPDS files (Joint Committee of Powder Diffraction Spectrometry).

The infrared absorption spectra were recorded using a SHIMADZU spectrometer (IR Affinity_1S, Fourier Transform Infrared Spectrophotometer) on a solid film in the form of a KRr pellet, where the treated compound was in suspension.

The DTA/TGA thermal analysis device was performed by SHIMADZU type (DTG – 60H). The tests were carried out with a heating/cooling rate of 10 °C/min. The scanning electron microscopy device was performed by FEI SEM Quanta type.

RESULTS AND DISCUSSION

Test 1: effect of pH on nickel removal in a mixture with an equimolar ratio 1[S$^=$]:1[Ni^{2+}]

In order to ensure a good precipitation of nickel ions, it is necessary to study the effect of different initial pH values on the nickel removal rate. The pH values have been defined based on many studies on sulfide precipitation (Reis *et al.* 2013; Li *et al.* 2019).

Diagrams illustrated in Figure 1 show the variation of Ni^{2+} ions concentration of synthetic and industrial solutions and their pH with time.

For both solutions, pH increases over time because of the consumption of S$^=$ to NiS at one time, and the release of H$_2$S gas, accelerated by the mechanical agitation, at the other time.

This observation was also revealed by researchers who worked on the treatment of synthetic nickel solution. They report that the pH of the nickel solution increased to approximately 9 as the reaction occurred (Karbanee *et al.* 2008; Reis *et al.* 2013). For initial pHs of 3 and 5 we note a remarkable decrease of nickel ions concentration for both solutions (Figure 1(b) and 1(d)), but for pHs of 6 and 7, this decrease is low. The yields of abatement at 25 minutes of reaction are presented in Table 1.

For industrial effluent, as can be seen in Figure 1(b), the nickel sulfide precipitation increased when pH reached 5. At this pH value, above 90% nickel ions were precipitated. Normally, in acidic solutions, S$^=$ is sufficiently present. Then, it can react easily with Ni^{2+} (reaction (3)). In the basic environment, reaction (2) is dominant; the preponderant species are HS$^-$ and H$_2$S. Thus, if the precipitation of NiS is not sufficient, all the more H$_2$S could evaporate with agitation as cited above. Nickel ions form complexes such as NiHS$^+$, Ni$_2$(HS)$^{3+}$ and Ni$_3$(HS)$^{5+}$, which probably involve the formation of NiS (Rickard *et al.* 1996). Some studies have argued that only HS$^-$ ions are responsible for the precipitation of NiS because S$^=$ ions are not present in sufficient concentration in the pH interval of 0–14 (Lewis & Van Hille 2006).

In both solutions (synthetic and industrial), the chemical precipitation of nickel was better at an initial pH of 5. However, the kinetics of reaction remained different. It was relatively weak for the industrial solution. This can probably be explained by the formation of complex molecules between Ni^{2+} and organic or mineral entities present in the industrial solution, thereby reducing accessibility of cations presumably because of their chelation, as confirmed by some authors (Wang *et al.* 2005; Jiang *et al.* 2008; Aghazadeh-Ghomi *et al.* 2018).

Test 2: effect of the ratio 1.5 [S$^=$]:1[Ni^{2+}] on the removal of Ni^{2+} at pH 5

Tests carried out with a ratio [S$^=$]/[Ni^{2+}] equal to 1.5/1 at pH 5 showed that the excess of sulfide ions reduced the efficiency of nickel removal (Figure 2).

The elimination yields of nickel ions, obtained in super saturation conditions after 25 minutes of reaction were 62% for the industrial solution (compared with 91% for tests carried out with a ratio 1[S$^=$]/1[Ni^{2+}]) and 92% for the synthetic solution (compared with 94% for 1[S$^=$]/1[Ni^{2+}]).

The decrease of nickel removal efficiency can be explained by a redissolution of the precipitate NiS, as demonstrated by some authors (Hille *et al.* 2005), or by the displacement of the equilibrium to more HS$^-$ and H$_2$S. This tendency, possibly enhanced by the rapid increase of pH, is related to the formation of aqueous polysulfide complexes or to the low stability of the fine sulfide particles.
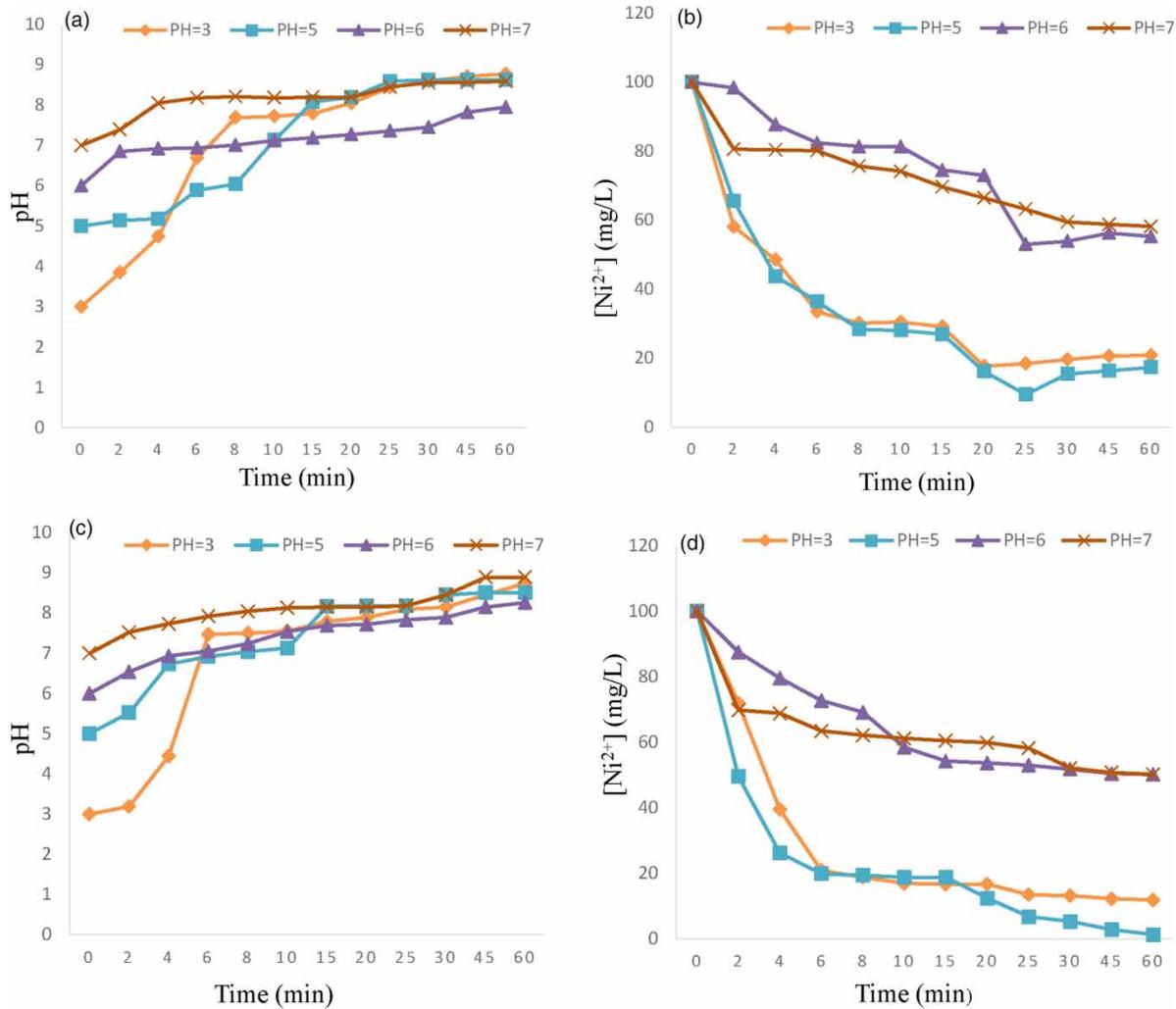
Figure 1 │ Variation of pH and Ni^{2+} concentration in the industrial effluent (a) and (b) and the synthetic solution (c) and (d) during chemical precipitation.

Table 1 │ Yields of nickel elimination

pH	3	5	6	7
Synthetic solution	86.56%	93.28%	47.08%	41.85%
Industrial solution	81.62%	90.63%	47.02%	36.83%

Studies performed by some authors on a synthetic solution ($[Ni^{2+}] = 200$ mg/L) of $NiSO_4$ in a ratio $[S^=]/[Ni^{2+}]$ of 1.5/1 show that excess sulfide produces nickel–sulfide complexes (stable at pH values above 7) (Uther *et al.* 1999; Karbanee *et al.* 2008). For the $1.5[S^=]/1[Ni^{2+}]$ ratio, the pH increases rapidly in the industrial effluent, after 2 minutes of reaction, from 5 to 7.89. This results probably from the

production of H_2S gas in large quantities because of the added amount of $S^=$ ions and its evacuation by stirring. Thereafter, pH stabilizes and reaches values identical to those obtained in tests carried out with a ratio of $1[S^=]/1[Ni^{2+}]$.

Test 3: influence of sulfide concentration on the removal of Ni^{2+} at pH = 5

Figure 3 shows the effect of sulfide concentration on the final concentration of nickel and the final pH of the industrial effluent.

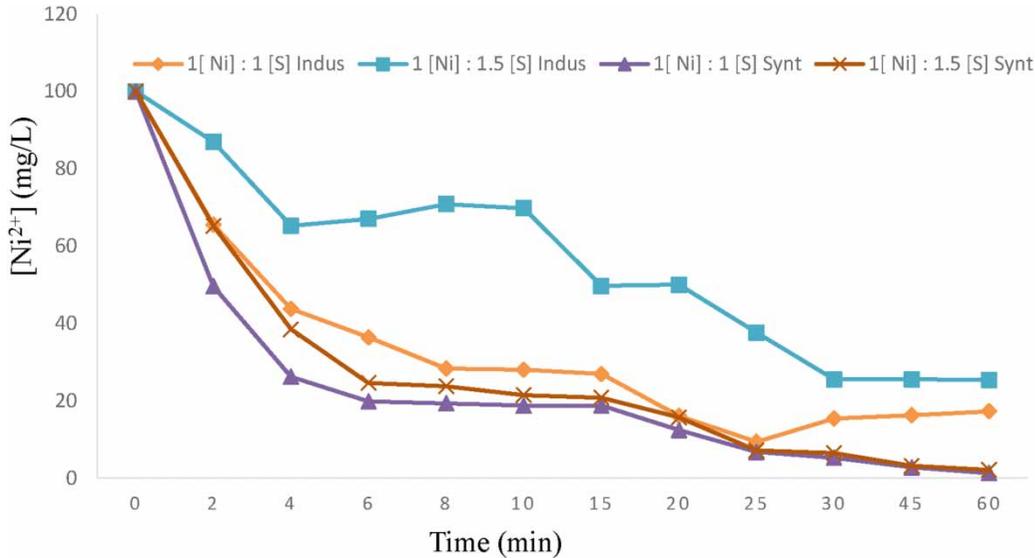The residual Ni^{2+} ions concentration decreases to a minimum corresponding to $S^=$ concentration of 33.33 mg/L

Figure 2 │ Effect of super saturation ($[S^=]/[Ni^{2+}]$ equal to 1.5/1) on nickel removal in the industrial and synthetic solution at pH 5.
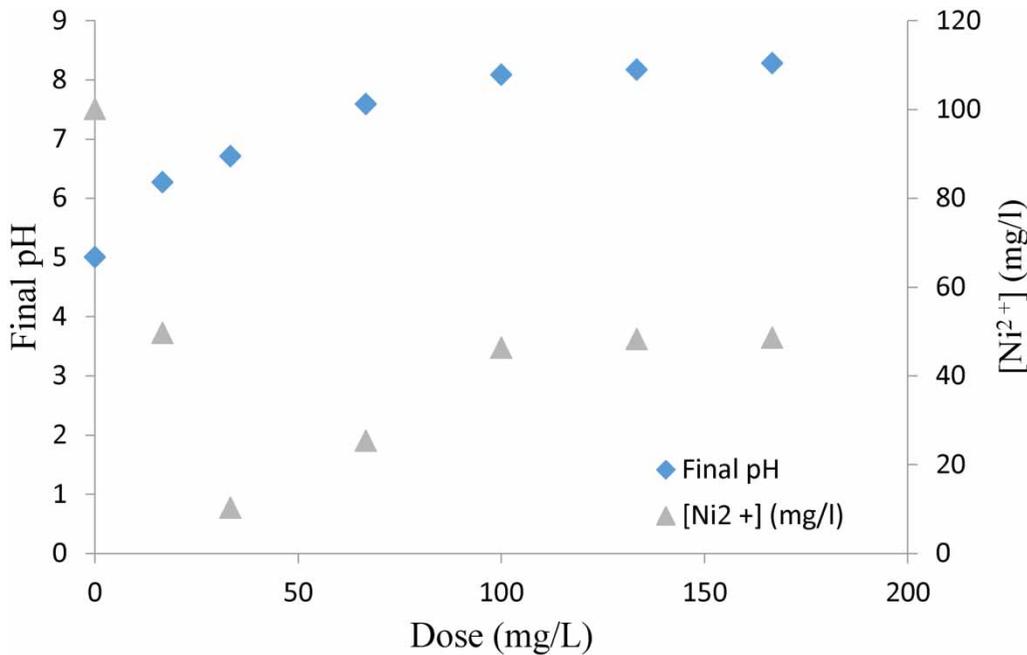

Figure 3 │ Effect of sulfide dose on nickel removal and the final pH of the industrial effluent.

(elimination yield of 84%) and a final pH of 5.6, then it increases, denoting a redissolution because of the increase of sulfide ions.

Examination of conductivity results shows:

- first, a decrease from 2.5 mS/cm to 0.7 mS/cm when the concentration of $S^=$ increases (34 mg/L), which could be

explained by the rise of concentration of Ni^{2+} by precipitation;

- then, an increase with the sulfide dose to reach 2.7 mS/cm approximately owing to the re-ionization, in the form of complexes $[Ni_x(HS^-)_y]^{(y-x)-}$;

- a minimum value of 0.7 mS/cm coinciding with that of the residual concentration of Ni^{2+}.

Characterization of nickel sulfide sludge

XRD spectra

The structure of the sludge issuing from the industrial effluent at optimal conditions of precipitation was studied using X-ray diffraction technique. The sludge has been heat treated at 190 °C, 350 °C and 600 °C. At 190 °C, the XRD diagram shown in Figure 4(a) illustrates an amorphous structure or poorly crystallized precipitate of nickel monosulfide. It should be noted that the number of diffraction lines is 7, with low intensities. It seems that the precipitate corresponds to the millerite (NiS). This could be supported by the works of some authors who have reported that the precipitate of nickel sulfide is an amorphous material (Dusastre *et al.* 1997; Jeong & Manthiram 2001). Similarly, another study reports identical results for a mixture of sulfide precipitates and confirms that they consisted of an amorphous NiS (Donges 1942).

Recent studies suggest that potential forms of nickel sulfide formed at low temperatures are β-NiS (millerite), NiS_2 (vaesite), Ni_3S_4 (polydymite) and Ni_3S_2 (heazlewoodite) (Bijmans *et al.* 2009; Sampaio *et al.* 2010; Reis *et al.* 2013). Authors suggest that the majority of these precipitates have a structure of millerite which is transformed into Ni_3S_4 (polydymite), accompanied by the production of the form Ni_3S_2 (heazlewoodite).

Thermic treatment at 350 °C affects the crystalline structure of the nickel sulfide, as observed in Figure 4(b). The X-ray spectrum shows the same lines appearing in that of the precipitate treated at 190 °C, but with more intense peaks. Diffraction peaks in Figure 4 were identified using the standard XRD of NiS from the JCPDS database (JCPDS – No.75-0613).

In Figure 4(c), at 600 °C, nickel oxide (NiO) is formed by oxidation of NiS as shown in reaction (5):

$$NiS(s) + 3/2 O_2(g) NiO(s) + SO_2(g) \rightarrow \tag{5}$$

The observed positions and planes of the formed product are in good agreement with the standard values of JCPDS database (No. 47-1049), indicated for NiO.

At high temperature, metallic elements have probably similar affinities for sulfide and have much higher affinities for oxygen, which explains the oxidation of sulfides in the presence of oxygen.

In a work on selective oxidation and sulfation of nickel concentrate, as a new technique for nickel production, it has been argued that in a roasting temperature ranging from 500 °C to 800 °C, the resulting product would be NiO (Yu *et al.* 2014). A recent study on the manufacture of nickel sulfides reports that in the presence of oxygen, the atoms of sulfides are rapidly replaced by the oxygen atoms to form nickel oxide (Balayeva *et al.* 2016).

Scanning electron microscopy

The characterization of the morphology of the thermally treated millerite at 190 °C, 350 °C and 600 °C was carried out using the SEM technique with similar dimensions.

The precipitate treated at 190 °C is poorly crystallized (Figure 5(a)). Otherwise, when the temperature is 350 °C, it appears as luminous aggregates with high polydispersity (Figure 5(b)). The grains or nanocrystals are characterized by a porous structure and are formed by agglomeration of small particles having irregular shapes and sizes, which gives the product a large exchange surface and can be used in electrocatalytic activities (Lin 2015). SEM photomicrographs support the morphological aspects of the millerite revealed in the previous sections.

For nickel sludge treated at 600 °C, micrographs in Figure 5(c) show that this compound has a structure formed from an assembly of aggregates similar to that observed in the literature for nickel oxide in its thin form.

Infrared spectroscopy

The identification of chemical structure and functional groups and bonds present in composants are well explored by infrared spectroscopy (Alamgholiloo *et al.* 2020).

Figures 6 and 7 show the infrared spectra obtained for sulfide sludge at treatment temperatures of 350 °C and 600 °C.

The wide peak at 3,465.5 cm^{-1} corresponds to the valence vibration of the O-H bond of water. The band which appears around 1,600 cm^{-1} is attributed to the angular deformation of H-O-H. As for the band located at 1,140 cm^{-1}, it characterizes the valence vibrations of the
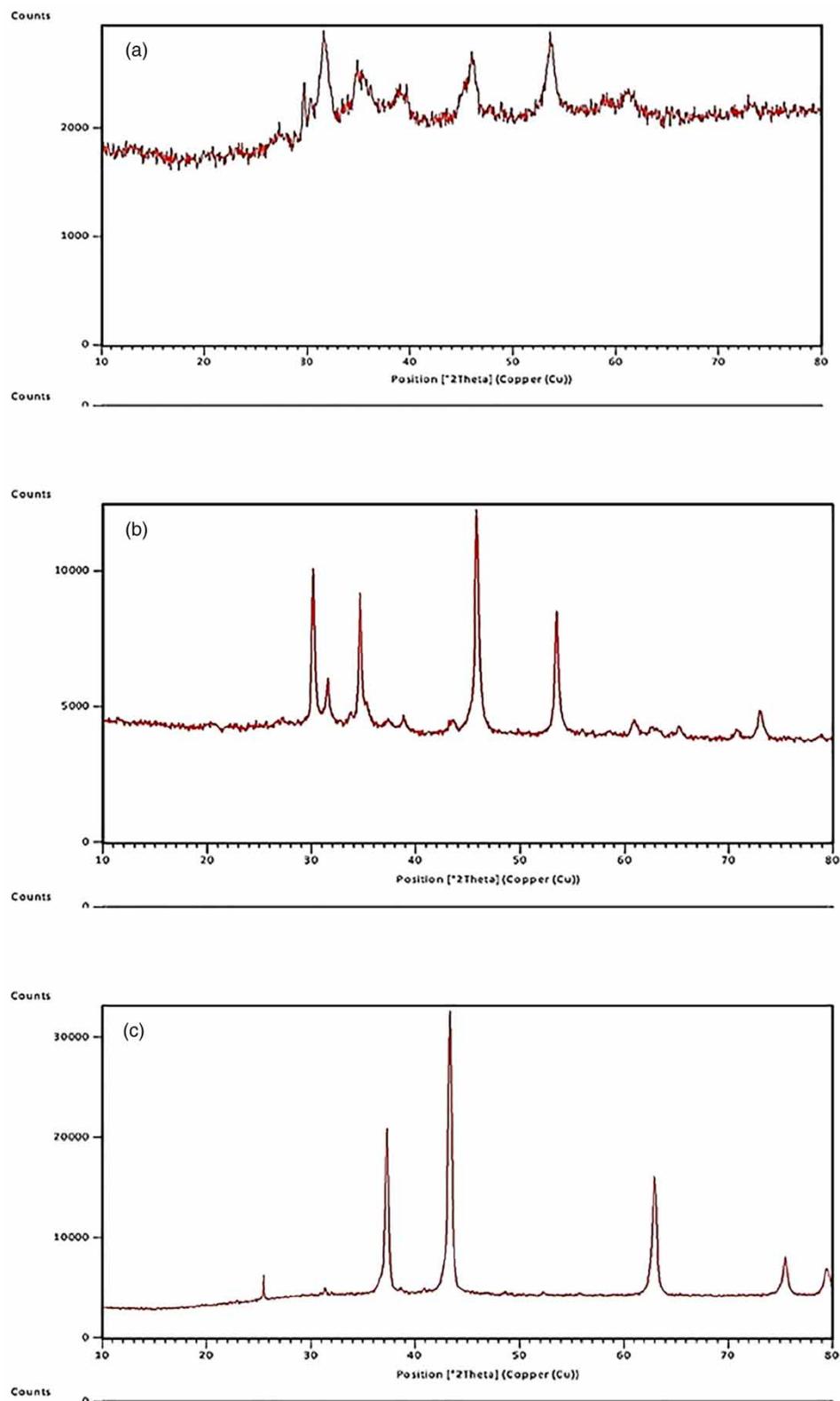
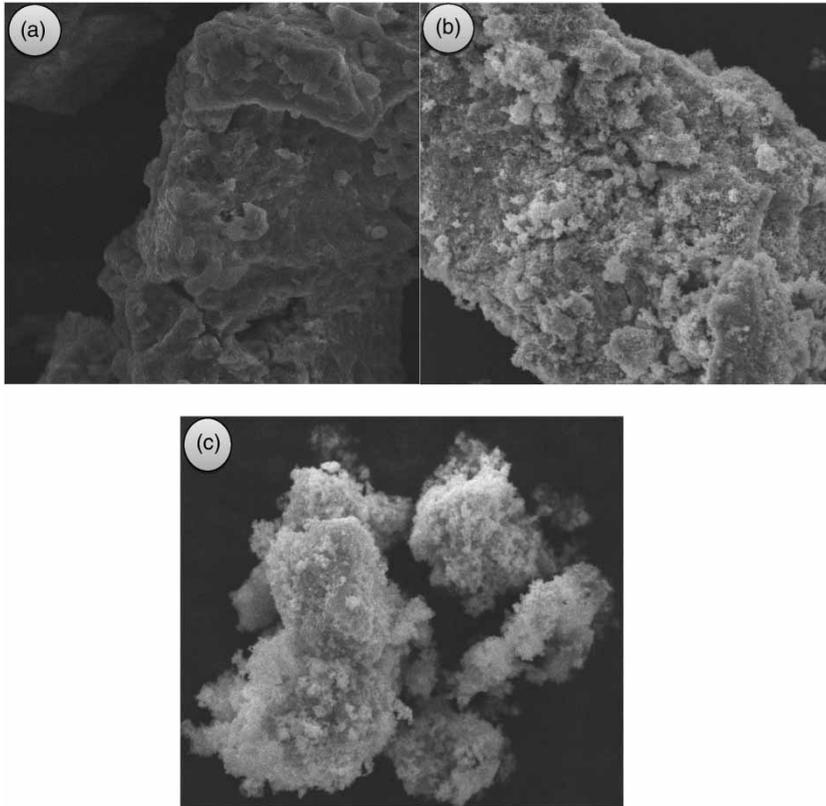**Figure 4** | Diffractogram of the treated nickel precipitate at (a) 190 °C, (b) 350 °C and (c) 600 °C.

Figure 5 | Scanning electron micrograph of NiS at (a) 190 °C (20 μm), (b) 350 °C (20 μm) and (c) 600 °C (20 μm).
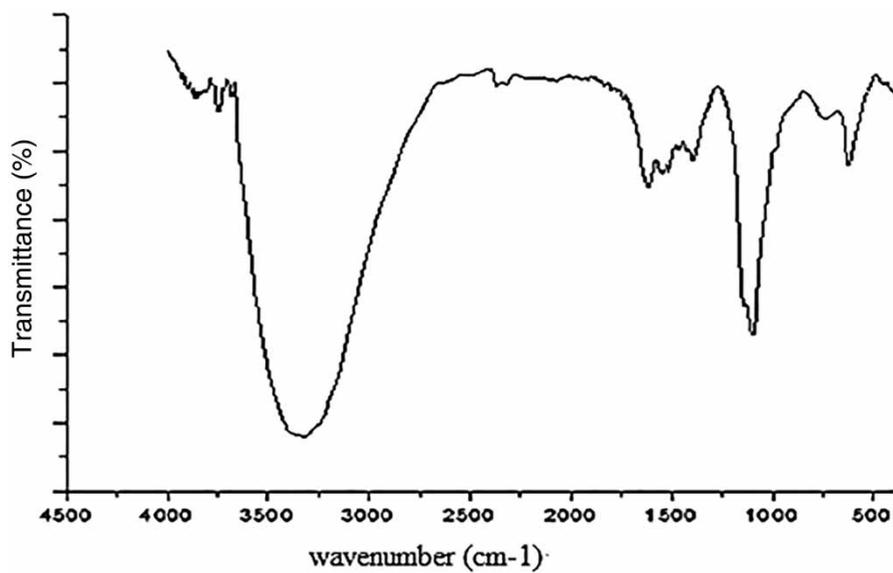

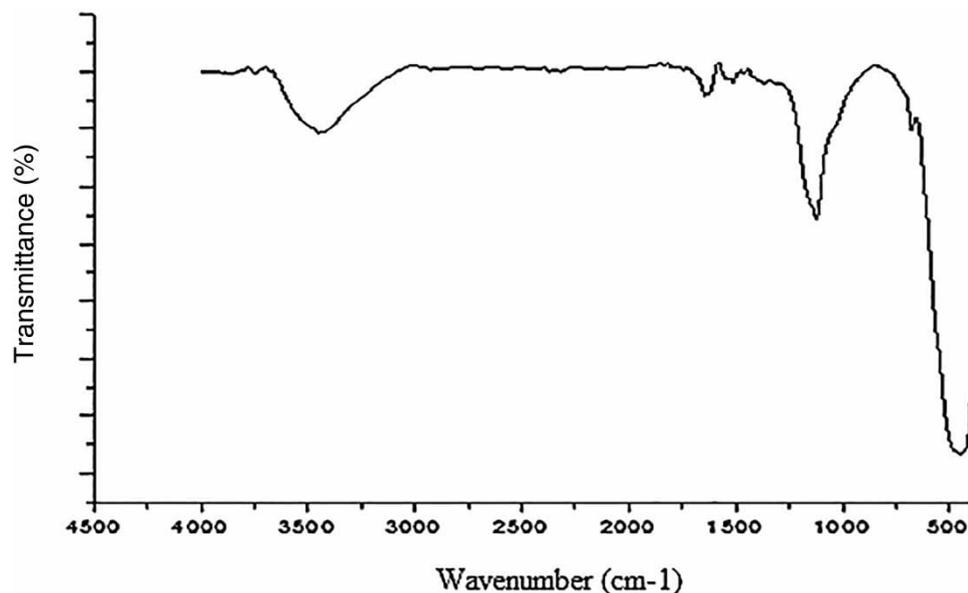**Figure 6** | IR spectrum of sulfide sludge heat treated at 350 °C for 24 hours.

Figure 7 │ IR spectrum of sulfide mud heat treated at 600 °C for 24 hours.

SO_4^{2-}. The least intense peak located at around 600 cm^{-1} reveals the presence of the Ni-S bond (Figure 6).

In Figure 7, we observe characteristic bands of the vibration of the hydration water located at 3,480 cm^{-1} and 1,600 cm^{-1}. The band that appears around 1,150 cm^{-1} is attributed to the valence vibration of the SO_4^{2-} molecule. As for the band located around 1,600 cm^{-1}, it is attributed to the angular deformation of H-O-H. The less intense peak around 600 cm^{-1} reveals the presence of an Ni-S bond. The band located around 500 cm^{-1} is probably due to the valence vibration of the Ni-O bond.

Thermal analysis

On the TGA curve, we detected three transformations (Figure 8):

- The first and second mass loss, between 43 °C and 426 °C, are due to water departure. At 426 °C the sludge dehydrates completely.
- The third mass loss is probably due to SO_2 molecules' departure. This transformation, which takes place between 522 °C and 555 °C, can be explained by reaction (6):

$$2\,NiS + 3\,O_2\ 2NiO + 2\,SO_2 \rightarrow \tag{6}$$
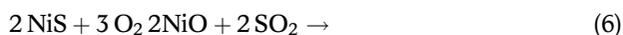
The DTA diagram highlights the following observations:

- A first exothermic peak around 170 °C probably corresponds to an allotropic transformation, transition from millerite apha (NiSα) to millerite beta (NiSβ).
- A second exothermic peak with low amplitude, located at 411 °C, is probably due to the crystallization of NiS.
- A third exothermic peak with large amplitude at 557 °C corresponds to a very energetic reaction. In the presence of oxygen from the air, nickel sulfides NiS transform into nickel oxide according to the following reaction:

$$2\,NiS + 3\,O_2\ 2NiO + 2\,SO_2 \rightarrow \tag{7}$$
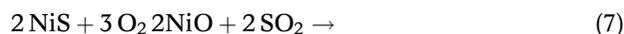
Nickel sulfide is known as a high performance catalyst. This material has a wide industrial application in hydrogenation reactions, in petrochemical and refining processes for the conversion of diolefins into mono-olefins to prevent the formation of gums and resins (Olivas *et al.* 1998). It has been proven as a bifunctional cathode electrocatalyst material for non-aqueous lithium-air batteries (LABs). NiS catalysts give a much better performance in terms of the specific capacity, discharge/charge overpotentials, rate dischargeability and cycling performance (Ma *et al.* 2015). NiO appears in the manufacturing of several products such as adhesives,
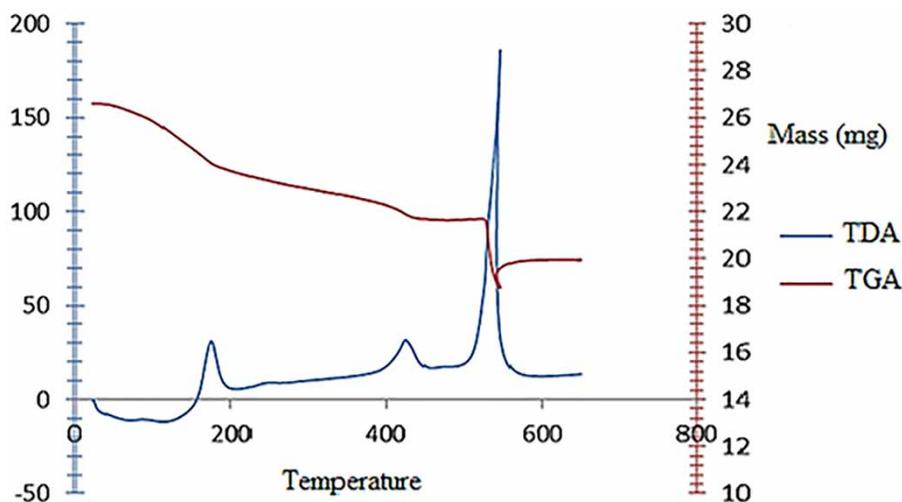
Figure 8 | TGA/DTA analysis of the sludge dried for 24 hours.

pigments for ceramics and glasses, and antiferromagnetic layers (Danjumma & Yakubu 2019).

CONCLUSION

The conducted research on the sulfide precipitation treatment of nickel-rich water has provided comprehension of the phenomenon occurring during the process. The results illustrated that the nickel removal efficiency depends on several parameters, such as the pH of the solution, the molar ratio $[S^=]/[Ni^{2+}]$ and the $S^=$ dosage. The removal yield achieved is approaching 90% for 25 minutes of treatment in the industrial effluent. The initial pH of 5 gave the best yields of nickel removal in the synthetic and industrial solutions. The effect of the sulfide dose on the removal of nickel from the industrial effluent was evaluated. XRD, IR, SEM, and TGA/DTA analysis reveal that the majority of products formed are NiS and NiO.

DATA AVAILABILITY STATEMENT

All relevant data are included in the paper or its Supplementary Information.

REFERENCES

Aghazadeh-Ghomi, M., Javad, M. & Naghi-Parvini, A. 2018 Enhanced selectivity of hydrolytic precipitation of Zn from Zn-Ni sulfate solution via chelation of Ni. *Trans. Nonferr. Metal. Soc.* **28** (12), 2566–2573. doi:10.1016/S1003-6326(18)64903-9.

Alamgholiloo, H., Rostamnia, S., Zhang, K., Lee, T. H., Lee, Y. S., Varma, R. S., Jang, H. W. & Shokouhimehr, M. 2020 Boosting aerobic oxidation of alcohols via synergistic effect between TEMPO and a composite Fe_3O_4/Cu-BDC/GO nanocatalyst. *ACS Omega* **5** (10), 5182–5191. doi:10.1021/acsomega.9b04209.

Babu, B., Ramesh, S., Udaya, B. & Seeni-Meera, K. 2009 Waste minimization in electroplating industries: a review. *J. Environ. Sci. Health* **27** (3), 155–177. doi:10.1080/10590500903124158.

Balayeva, O., Abdulsaid, A., Azizov-Mustafa, B., Muradov, A., Goncha, M., Rasim, M., Alosmanov-Zamin, Q. & Aghamaliyev, Z. 2016 β-NiS and ni₃s₄ nanostructures: fabrication and characterization. *Mater. Res. Bull.* **75**, 155–161. doi:10.1016/j.materresbull.2015.11.037.

Bijmans, M., Helvoort, P. J. V., Dar, S. A., Dopson, M., Lens, P. N. L. & Buisman, C. J. N. 2009 Selective recovery of nickel over iron from a nickel–iron solution using microbial sulfate reduction in a gas-lift bioreactor. *Water Res.* **43** (3), 853–861. doi:10.1016/j.watres.2008.11.023.

Binet, M. T., Adams, M. S., Gissi, F., Golding, L. A., Schlekat, C., Garman, E., Merrington, G. & Stauber, L. J. 2018 Toxicity of nickel to tropical freshwater and sediment biota: a critical literature review and gap analysis. *Environ. Toxol. Chem.* **37** (2), 293–317. doi:10.1002/etc.3988.

Brbooti, M., Balasim, A. & Al-shuwaiki, N. 2011 Removal of heavy metals using chemicals precipitation. *Eng. Technol. J.* **29** (3), 595–612.

Cao, J., Zhang, G., Mao, Z., Fang, Z. & Yang, C. 2009 Precipitation of valuable metals from bioleaching solution by biogenic sulfides. *Miner. Eng.* **22** (3), 289–295. doi:10.1016/j.mineng.2008.08.006.

Coman, V., Robotin, B. & Ilea, P. 2013 Nickel recovery/removal from industrial wastes: a review. *Resour. Conserv. Recy.* **73** (2013), 229–238. doi:10.1016/j.resconrec.2013.01.019.

Danjumma, S. G. & Yakubu, A. 2019 Nickel oxide (NiO) devices and applications: a review. *Inter. J. Eng. Res. Tech.* **8** (4), 2–9.

Donges, V. 1942 Zur Säurelöslichkeit von Gefalltem Kobalte Und Nickelsuifidl (The acidity of cobalt and nickel sulfide). *Zeit. Anorgan Chemie* **253** (5–6), 345–351. doi:10.1002/zaac.19472530512.

Dusastre, V., Bashe, O., Ivan, P. P. & Graham, A. S. 1997 Convenient, room-temperature, amine-assisted routes to metal sulfides, selenides and tellurides. *J. Chem. Soc. Dalton. Trans.* **19**, 3505–3508. doi:10.1039/A702833D.

Hille, V., Robert, P., Peterson, K. A. & Alison, E. L. 2005 Copper sulphide precipitation in a fluidised bed reactor. *Chem. Eng. Sci.* **60** (10), 2571–2578.

Jeong, Y. U. & Manthiram, A. 2001 Synthesis of nickel sulfides in aqueous solutions using sodium dithionite. *Inorg. Chem.* **40** (1), 73–77. doi:10.1021/ic000819d.

Jerroumi, S., Nagala, S., Lekhlif, B., Jamal, J. E. & Afrine, L. 2019 Investigation of electrocoagulation on the removal of nickel in waste water from an electroplating bath using aluminium and iron electrodes. *Mor. J. Chem.* **4** (5), 727–738.

Jiang, S., Fenglian, F., Junxiong, Q. & Ya, X. 2008 A simple method for removing chelated copper from wastewaters: Ca(OH)$_2$-based replacement-precipitation. *Chemosphere* **73** (5), 785–790.

Karbanee, N., Van Hille, R. & Lewis, A. 2008 Controlled nickel sulfide precipitation using gaseous hydrogen sulfide. *Indus. Eng. Chem. Res.* **47** (5), 1596–1602. doi:10.1021/ie0711224.

Lentini, P., Zanoli, L., Granata, A., Signorelli, S. S., Castellino, P. & Dell'Aquila, R. 2017 Kidney and heavy metals – the role of environmental exposure (review). *Mol. Med. Rep.* **15** (5), 3413–3419. doi:10.3892/mmr.2017.6389.

Lewis, A. E. 2010 Review of metal sulphide precipitation. *Hydrometallurgy* **104** (2), 222–234. doi:10.1016/j.hydromet.2010.06.010.

Lewis, A. & Van Hille, R. 2006 An exploration into the sulphide precipitation method and its effect on metal sulphide removal. *Hydrometallurgy* **81** (3–4), 197–204. doi:10.1016/j.hydromet.2005.12.009.

Li, H., Hongguo, Z., Jianyou, L., Ping, Z. & Yongheng, C. 2019 Combined Fenton process and sulfide precipitation for removal of heavy metals from industrial wastewater: bench and pilot scale studies focusing on in-depth thallium removal. *Front. Env. Sci. Eng.* **13** (4), 1–12. doi:10.1007/s11783-019-1130-7.

Lin, J. Y. 2015 Nickel sulfide counter electrodes enhanced by hydrosulphuric acid hydrothermal treatments for use in Pt-Free. *Electrochim. Acta* **155** (2), 103–109. doi:10.1016/j.electacta.2015.01.004.

Ma, Z., Yuan, X., Zhang, Z., Mei, D., Li, L., Ma, Z. F., Lei, Z., Jun, Y. & Jiujun, Z. 2015 Novel flower-like nickel sulfide as an efficient electrocatalyst for non-aqueous lithium-air batteries. *Sci. Rep.* **5** (12), 1–9. doi:10.1038/srep18199.

Mnasri-Ghnimi, S. & Frini-Srasra, N. 2019 Removal of heavy metals from aqueous solutions by adsorption using single and mixed pillared clays. *Appl. Clay. Sci.* **179** (5), 105–151. doi:10.1016/j.clay.2019.105151.

Olivas, A., Cruz-Reyes, J., Petranovskii, V., Avalos, M. & Fuentes, S. 1998 Synthesis and characterization of nickel sulfide catalysts. *J. Vac. Sci. Technol. A* **16** (6), 3515–3520.

Pan, Z. F. & An, L. 2019 Removal of heavy metal from wastewater using ion exchange membranes. In: *Applications of Ion Exchange Materials in the Environment* (M. I. A. Inamuddin & A. M. Asiri eds). Springer Nature, Cham, Switzerland.

Panepinto, D., Silvia, F., Giuseppe, G. & Marco, A. 2016 Thermal valorization of sewer sludge: perspectives for large wastewater treatment plants. *J. Clean. Prod.* **137** (1), 1323–1329. doi:10.1016/j.jclepro.2016.08.014.

Reis, F. D., Silva, A. M., Cunha, E. C. & Leao, V. A. 2013 Application of sodium- and biogenic sulfide to the precipitation of nickel in a continuous reactor. *Sep. Purif. Technol.* **120** (2013), 346–353. doi:10.1016/j.seppur.2013.09.023.

Rickard, D. T., Theberge, S. & Olroyd, A. 1996 Determination of metal (Bi) sulfide stability constants of Mn^{2+}, Fe^{2+}, Co^{2+}, Ni^{2+}, Cu^{2+} and Zn^{2+} by voltammetric methods. *Environ. Sci. Technol.* **30** (2), 671–769.

Sampaio, R., Timmers, R., Xu, Y., Keesman, K. J. & Lens, P. N. L. 2009 Selective precipitation of Cu from Zn in a PS controlled continuously stirred tank reactor. *J. Hazard. Mater.* **165** (1–3), 256–265.

Sampaio, R. M. M., Timmers, R. A., Kocks, N., André, V., Duarte, M. T., Hullebusch, E. D. V., Farges, F. & Lens, P. N. L. 2010 Zn-Ni sulfide selective precipitation: the role of supersaturation. *Sep. Purif. Technol.* **74** (1), 108–118.

Shi, S., Xu, G., Yu, H. & Zhang, Z. 2018 Strategies of valorization of sludge from wastewater treatment. *J. Chem. Technol. Biotechnol.* **93** (4), 936–944. doi:10.1002/jctb.5548.

Sunder, S. G., Adhikari, S., Rohanifar, A., Poudel, A. & Kirchhoff, J. R. 2020 Evolution of environmentally friendly strategies for metal extraction. *Separations* **7** (1), 1–27. doi:10.3390/separations7010004.

Taouil, H., Ibn ahmed, S., El Assyry, A., Hajjaji, N. & Srhiri, A. 2014 Evaluation of metal pollution: aluminum, zinc, iron and copper of Tiykomiyne well water (East Morocco). *J. Mat. Environ. Sci.* **5** (1), 177–182.

Uther, G., Heberge, S., Stephen, M. T., Heberge, W. & David, T. R. 1999 Sulfides evidence for aqueous clusters as intermediates during zinc sulfide formation. *Geochim. Cosmochim. Acta* **63** (19), 3159–3169.

Wakida, F. T., Lara-Ruiz, D., Temores-Peña, J., Rodriguez-Ventura, J. G., Diaz, C. & Garcia-Flores, E. 2008 Heavy metals in sediments of the Tecate River, Mexico. *Environ. Geol.* **54** (3), 637–642.

Wang, J. & Chen, C. 2015 The current status of heavy metal pollution and treatment technology development in China. *Environ. Technol. Rev.* **4** (1), 39–53. doi:10.1080/21622515.2015.1051136.

Wang, L. K., Hung, Y. T. & Shammas, N. K. 2005 *Physicochemical Treatment Processes*. Humana Press Inc, Totowa, NJ, USA.

Wei, J., Duan, M., Li, Y., Nwankwegu, A. S., Ji, Y. & Zhang, J. 2019 Concentration and pollution assessment of heavy metals within surface sediments of the Raohe Basin, China. *Sci. Rep.* **9** (1), 1–7. doi:10.1038/s41598-019-49724-7.

Wu, R. 2019 Removal of heavy metal ions from industrial wastewater based on chemical precipitation method. *Ekoloji* **28** (107), 2443–2452.

Xu, G., Xin, Y. & Spinosa, L. 2015 Development of sludge-based adsorbents: preparation, characterization, utilization and its feasibility assessment. *J. Environ. Manag.* **151** (2015), 221–232. doi:10.1016/j.jenvman.2014.08.001.

Yu, D., Torstein, A. U. & Barati, M. 2014 Fluidized bed selective oxidation and sulfation roasting of nickel sulfide concentrate. *Metall. Mater. Trans. B* **45** (10), 653–661. doi:10.1007/s11663-013-9958-x.

Zelekew, O. A. & Kuo, D. H. 2017 Synthesis of a hierarchical structured NiO/NiS composite catalyst for reduction of 4-nitrophenol and organic dyes. *RSC Advances* **7** (8), 4353–4362.